PHYSICAL REVIEW E **89**, 012815 (2014)

Rubik's cube: An energy perspective

Yiing-Rei Chen
Department of Physics, National Taiwan Normal University, Taipei 11677, Taiwan

Chi-Lun Lee*
Department of Physics, National Central University, Jhongli 32001, Taiwan

(Received 16 October 2013; published 29 January 2014)

What if we played the Rubik's cube game by simple intuition? We would rotate the cube, probably in the hope of getting a more organized pattern in each next step. Yet frustration occurs easily, and we soon find ourselves trapped as the game progresses no further. Played in this completely strategy-less style, the entire problem of the Rubik's cube game can be compared to that of complex chemical reactions such as protein folding, only with less guidance in the searching process. In this work we look into this random-searching process by means of thermodynamics and compare the game's dynamics with that of a faithful stochastic model constructed from the statistical energy landscape theory (SELT). This comparison reveals the peculiar nature of SELT, which relies on the random energy approximation and often chops up energy correlations among nearby configurations. Our observation provides a general insight for the use of SELT in the studies of these frustrated systems.

DOI: 10.1103/PhysRevE.89.012815 PACS number(s): 82.20.−w

I. INTRODUCTION

Rubik's cube has drawn long-lasting interest from the general public as well as the scientific community since its birth in the 1970s [1]. The cube itself bears a concise physical structure and is operated with basic rotational rules. Yet it appears difficult for most players to solve the cube toward its ultimate, ordered pattern. The vast number of configurations (of the order of 10^{19}), along with the rotations that serve as their links, form a network that has a regular structure, in the sense that each configuration is linked to an identical number of nearest neighbors. In spite of the numerous configurations, it has been proven recently that the shortest path between any two configurations contains no more than 20 steps [2], each step standing for a rotation of some face by 90° or 180°, clockwise or counterclockwise [3].

Aside from the elegance of its mathematical structure [4], the Rubik's cube game, when played with a very naive attitude, leads to experiences that are strikingly similar to those with the famous protein-folding problem [5]. The similarity mainly lies in the frustration during the global minimum searching process, and this frustration is attributed to the lack of farsighted guidance and the misleading local traps. In the protein-folding problem, however, the searching process can be suddenly sped up as guided sequential moves are triggered, such as zipping or helical structure formation, which follows the so-called "cooperative" nature [6–8], an essence due to the chain-connecting structure in proteins. The lack of such essence in the Rubik's cube problem leads to a slower, more random searching process, where single rotations are often accompanied by huge energy leaps. In fact, following the commonly used Monte Carlo simulation procedure [9], for a standard $3 \times 3 \times 3$ Rubik's cube it is almost impossible to reach the ultimate pattern within a reasonable computing time. In the current study, we choose to use a simplified energy function that ignores the edge patches of the cube, so as to make computer simulations and energy landscape analysis [10,11] possible.

From our previous study [12], we have demonstrated that the Rubik's cube problem, if viewed from the thermodynamic perspective, exhibits a peak in heat capacity. This peak represents the existence of a transition between the native state, which represents the configuration for the energy optimum, and the disordered state, which stands for the vast number of disordered configurations. This feature alone bears a striking resemblance to the folding transition of the protein problem. Moreover, via Monte Carlo simulations we find that the mean first-passage time (MFPT) [13] exhibits a U-shaped trend versus temperature. This indicates that the searching process towards the native state gets much faster at the optimized temperature than an unguided search throughout the whole configuration space [14]. From a statistical study we have confirmed that the energy landscape has a bias towards the native state, while the nature for the frustrated landscape is best exhibited through a nonexponential relaxation in the energy autocorrelation function. All of these results coincide well with the corresponding observations in protein-folding research. Despite this analogy, we should point out that the Rubik's cube problem, having a highly simplified structure, possesses a relatively tiny funnel-like region in its energy landscape, which results in a more diffusive searching process than the protein-folding dynamics.

In the protein science community, studies concerning such bumpy energy landscapes are often performed with the aid of the statistical energy landscape theory (SELT) [10,15], where the numerous configurations as well as their detailed reaction links are parameterized by one or a few reaction coordinates. After being projected onto these reaction coordinates, the huge amount of configurational information is transformed into a statistical distribution that establishes the stochastic nature of the theoretically rebuilt model, which features a random energy Hamiltonian [16,17]. Originally developed for studies on protein folding without consideration of cooperativity [15,18], SELT is, in our perspective, a very promising tool for describing the Rubik's cube problem.

*chilun@ncu.edu.tw

In the spirit of methodologic study, we construct SELT in the current work as a rebuilt version of the Rubik's cube model (RCM) we use, and examine the similarity and dissimilarity between the two. Regarding the MFPT, the Monte Carlo simulations performed for both models show the same qualitative features that characterize the protein-folding dynamics. In particular, the MFPT results from both models agree well quantitatively in the high-temperature regime. To understand the numerical discrepancy that increases at low temperatures, we examine the energy-time series and find the frozen movements peculiar to the random walker of SELT. We point out from there the essential difference between the dynamic behaviors with the two models. In short, while RCM's random walker pays more short-term visits to secondary minima, SELT's random walker seldom encounters the "trap states" but gets frozen there once it steps in. Moreover, the entrapment in SELT is both energetic and entropic, which leads to a very different temperature dependence in its dynamic behavior.

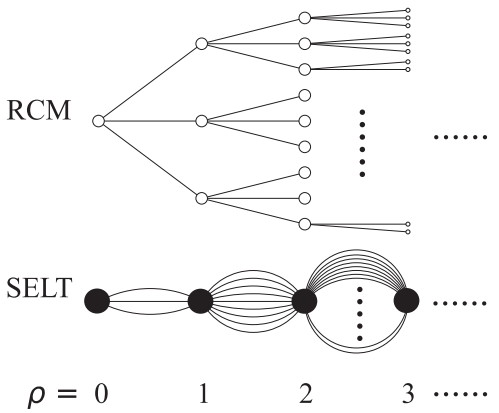

FIG. 1. Illustration for the network-structure comparison of RCM versus SELT. In SELT, configurations of the same ρ are combined into one supernode, and each configuration of ρ is connected to all configurations of $\rho \pm 1$.

II. MODELS AND METHODS

In this work we use a simplified $3 \times 3 \times 3$ RCM, where we ignore the edge patches and only consider the colors of corner patches and face-center patches in the energy function. For each configuration of this model, the corresponding energy is defined by $E = -\sum_{i=1}^{6} n_i$, where the summation runs over all six faces of the cube, and n_i is the number of corner patches that sit on the ith face and share the same color with the central patch of that face. The lowest energy of the cube is therefore -24, which corresponds to the ultimate configuration where all six faces are solid colored. Following the language of protein-folding dynamics, we choose to call this ultimate configuration the "native state."

Once the energy function is defined, one can rephrase the Rubik's cube problem in the language of thermodynamics. In particular, its kinetic behavior under a constant-temperature heat bath can be established using the Metropolis Monte Carlo algorithm [9]. For each Monte Carlo time step, a move is picked from a total of 12 rotations, whereas a "rotation" means picking a face and rotating the layer of pieces underneath that picked face by 90°, clockwise or counterclockwise. Whether this move is actually performed is determined by the Metropolis algorithm, to assure the detailed-balance condition upon thermodynamic equilibrium. For simplicity, we use dimensionless units for energy and temperature and take $k_B \equiv 1$ for the Boltzmann constant.

To help grab a taste of the "game progress,' as if in protein-folding problems, we define an order parameter ρ that labels the distance, namely, the minimal number of rotations, towards the native state. The vast number of configurations of RCM can be classified by their ρ numbers, which are no larger than 14. Subsequently, statistical information such as the energy probability distribution $P(E,\rho)$ and the total number of links between successive ρ's can then be derived.

In particular, the projection from the configuration space onto the ρ axis leads us to the construction of SELT via the random energy approximation. In RCM, each specific rotation forms a link between a certain configuration of ρ and another of $\rho \pm 1$, with no ambiguity [19]. In other words, in the RCM network structure, the configurations work as nodes, and each node is linked by rotations to 12 neighbors. However, in SELT, the actual patterns of the configurations are intentionally suppressed, and so is the specificity of their links. All nodes of the same ρ merge to one supernode, while the same total number of links remain connected between supernode ρ and supernode $\rho \pm 1$ (please refer to Fig. 1). In doing so, the identities of links and configurations are no longer recognizable. The total numbers of links between ρ and $\rho \pm 1$, denoted by $l_{\pm}(\rho)$, should give what we call the connecting probability, $\lambda_{\pm}(\rho) = l_{\pm}(\rho)/[l_{+}(\rho) + l_{-}(\rho)]$.

We perform Monte Carlo simulations for SELT with the following algorithm: Starting from some "state" (rather than a "configuration") of certain ρ number and energy E, a random walker would choose to move forward or backward, according to the connecting probability $\lambda_{\pm}(\rho)$. The energy of this would-be-next step is stochastically generated thereon, by a random variable, $\mathcal{H}(\rho \pm 1)$, that follows the statistical profile $P(E, \rho \pm 1)$ extracted from RCM.

Therefore, on the one hand, we have the original RCM landscape, and on the other hand, with details smeared, we construct an artificial landscape of SELT according to the stochastic energy function. In this work we would like to use the Rubik's cube problem as a pivot to understand how well this SELT can approximate the RCM landscape.

Note that the essence of RCM is inherited by SELT in the form of $\lambda_{\pm}(\rho)$ and $\mathcal{H}(\rho \pm 1)$. With such a simplified probabilistic description, mean-field properties are inevitably presented in SELT to some extent. However, fluctuations beyond mean-field discussions are automatically generated by the stochastic nature of $\mathcal{H}$. In particular, note that while SELT has been widely used in predicting complex molecular dynamics, it is mainly performed with the aid of the master-equation (ME) approach. This approach enhances the mean-field feature of the system, as it replaces reactions via multiple pathways by simple averaged reaction constants. Since further insights will not be available until a faithful study beyond the ME approximation appears, in this work we choose to perform direct computer simulations instead, to extract more accurate information for the dynamics of SELT.

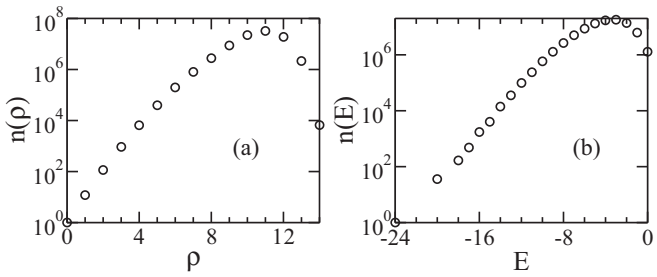

FIG. 2. Number of configurations versus (a) the order parameter ρ and (b) the energy in RCM.

III. RESULTS

The statistics of the RCM configurations, such as the energy probability distribution $P(E,\rho)$ and the connecting probability $\lambda_{\pm}(\rho)$, are acquired from our computer exhaustive studies that branch out from the native state. There are a total of 88 179 840 configurations for our simplified $3\times3\times3$ cube, and their statistic information versus ρ and E is plotted in Fig. 2. Note that the exponential growth near the native state, as revealed in Figs. 2(a) and 2(b), implies that low-energy (i.e., $E<-12$) or native vicinity configurations occupy only a very small fraction of the overall configuration space.

In RCM, the probability distributions of energy change for links between ρ and $\rho\pm1$ are denoted by $P^{\pm}_{\rm RCM}(\Delta E,\rho)$, as plotted in Fig. 3. The corresponding probability distributions

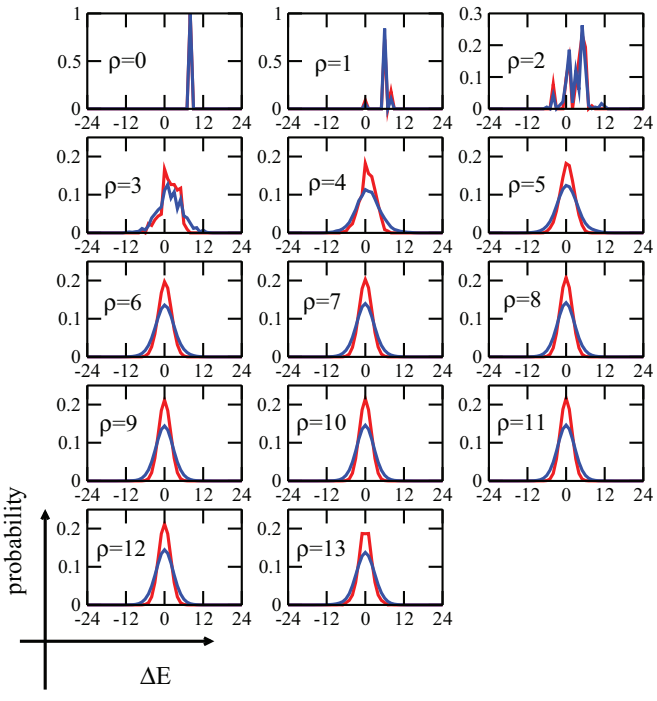

FIG. 3. (Color) Probability distributions over energy change. Only plots for forward motions of $\rho\to\rho+1$ are listed. As for backward motions of $\rho\to\rho-1$, the distribution is just the reflection of plot $\rho-1\to\rho$ over axis $\Delta E=0$. Red, RCM; blue, SELT.

in SELT are given by

$$P^{\pm}_{\rm SELT}(\Delta E,\rho)\equiv\sum_{E_1,E_2}P(E_1,\rho)P(E_2,\rho\pm1)\delta_{E_2-E_1,\Delta E}. \quad (1)$$

We see in Fig. 3 that for $\rho<3$ the probability distribution created in SELT shows little difference from that in RCM. Furthermore, the observation that both $P_{\rm RCM}(\Delta E,\rho)$ and $P_{\rm SELT}(\Delta E,\rho)$ resemble a Gaussian distribution for $\rho>3$ leads to an intuitive speculation that, despite the specificity in its configuration structure, RCM gives rise to such uncorrelated profiles for energy change between consecutive steps, and the random-energy hypothesis in SELT is, after all, well supported in this aspect. Nevertheless, by comparison we find that $P_{\rm SELT}(\Delta E,\rho)$ is, in general, broader then $P_{\rm RCM}(\Delta E,\rho)$, which manifests the artifact produced by stochastically assigned connections.

We now turn to a discussion of dynamics by first looking at the MFPT towards the native state. As derived in our previous work [12] on RCM simulations and the parallel study with an ME approximation, the MFPT curves exhibit a U-shaped feature (called "chevron rollover" in the studies of protein-folding dynamics [20]), and the slow dynamics in the high- and low-temperature regimes shown therein can be accounted for by the tedious random-searching process and the existence of deep energy traps, respectively. In the ME approximation [12], the dynamics is mapped to a one-dimensional diffusion process along ρ, where transitions between successive ρ's are represented by the average reaction rates,

$$k_{\rho,\rho\pm1}=\sum_{E}\sum_{E'}P(E,\rho)P(E',\rho\pm1)k(E\to E'), \quad (2)$$

and $k(E\to E')$ is the transition rate between two configurations via the Metropolis algorithm.

With the new MFPT result in this work, we first make a comparison between the ME approximation and SELT, in terms of how much they preserve and reveal for the dynamic message in RCM simulations. As shown in Fig. 4, the ME approach underestimates the reaction dynamics, especially at low temperatures. This can be easily explained: when the approach described in Eq. (2) is applied, the kinetics of all configuration links are averaged. Since deep energy traps are featured by low-rate, low-population processes, they fail to make any significant contribution to this average. (Alternatively, one may choose to derive for each ρ the leaving rate from the average waiting time, following what is done in the Bryngelson-Wolynes theory [18,21,22]. In that manner the dynamics of low-lying energy traps would be greatly amplified and result in a very slow diffusion process.)

To go beyond the mean-field approach of ME, direct SELT simulation should serve as a better approximation to RCM, since fluctuation of the kinetic rate is then considered. In fact, it is remarkable to see in Fig. 4 that the MFPT result of SELT fits much better to that of RCM in the high-temperature regime. However, the discrepancy between the two models increases significantly at low temperatures. Further study is therefore needed to resolve the dynamic distinction between the two models.

To look further into the dynamics, we now examine the average number of moves during the first-passage (FP) time,

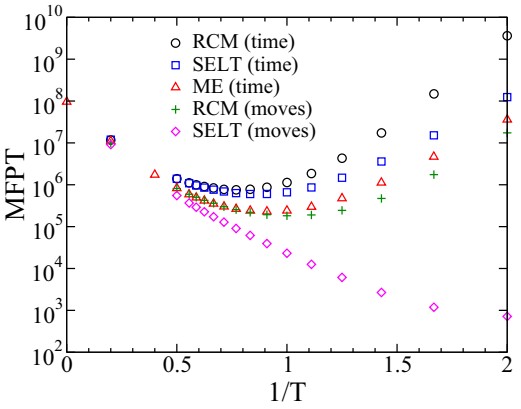

FIG. 4. (Color online) Results of the mean first-passage time (MFPT). Squares represent SELT data from direct simulations; data from RCM simulations (circles) and data from SELT predictions using the master-equation (ME) analysis (triangles) were derived previously [12] and are also shown here. Crosses and diamonds mark the average numbers of first-passage (FP) moves for RCM and SELT simulations, respectively. The average is performed for 10 000 simulations at each temperature for each model.

as shown in Fig. 4, for RCM and SELT. Note that a "move" is defined here as an actual change of configuration, and in our case, it is also equivalent to an actual change of the random walker's position on the order parameter axis. Surprisingly, while the RCM result still exhibits a U-shaped feature, the average number of moves in SELT shows a monotonic decrease with $1/T$. At $T = 0.5$ it even becomes less than 1000, almost in scale with the number of moves during the diffusive MFPT of a nonguided one-dimensional random walk.

The above observation reveals a curious fact, that while the random walker in SELT simulations appears to be slow at low temperatures, it actually spends considerably fewer moves searching for the native state. Figure 5 is a snapshot of the energy-time series for both simulations at $T = 0.7$. The random walker of SELT stays frozen most of the time and, therefore, gives far fewer details in its dynamics. In other words, the SELT simulations' success in mimicking the MFPT trend in RCM is in fact based on a very distinct dynamic behavior.

Energy-time series such as the one shown in Fig. 5 can be used to derive the autocorrelation function $C_E(t)$, defined by $C_E(t) = \langle \Delta E(t) \Delta E(0) \rangle / \langle \Delta E^2 \rangle$, where $\Delta E \equiv E - \langle E \rangle$. Serving as a memory function, $C_E(t)$ provides a clearer

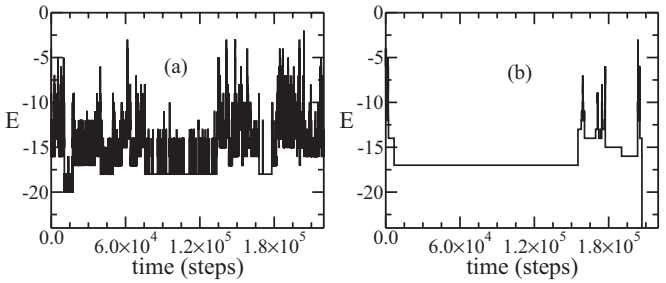

FIG. 5. Snapshots of the energy time series for (a) RCM and (b) SELT at $T = 0.7$.

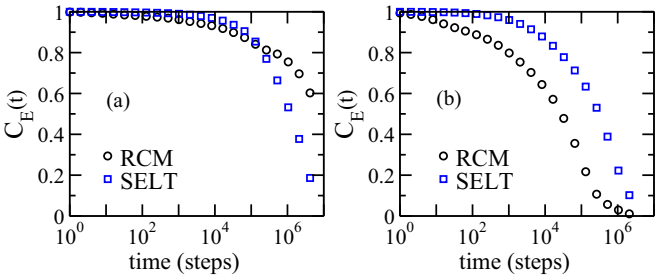

FIG. 6. (Color online) (a) Energy autocorrelation functions $C_E(t)$ for RCM (circles) and SELT (squares) at the equilibrium of $T = 0.7$. For each model, the values of $C_E(t)$ are obtained from a simulation of 10^{10} Monte Carlo time steps. (b) Energy autocorrelation functions at $T = 0.7$, acquired from 1000 FP simulations for both models.

perspective for understanding the essentials of the different dynamic behaviors. In particular, we show the results of $C_E(t)$ at $T = 0.7$, for equilibrium in Fig. 6(a) and for FP processes in Fig. 6(b). The legitimacy of the autocorrelation function in Fig. 6(b) is based on the equilibrium provided by the sampled FP cases. As a check, the FP average energy is $\langle E \rangle = -18.126$ for RCM and $\langle E \rangle = -18.121$ for SELT, both sitting closely to the number $\langle E \rangle = -18.125$, derived from the partition function excluding only the native state.

When the native state is excluded, as demonstrated in Fig. 6(b), SELT possesses a better memory on all time scales of interest. The differences between Fig. 6(a) and Fig. 6(b) are certainly due to the influence of the native state. By including this influence, the result of the long-term memory competition is reversed.

Note that in this example of a relatively low temperature, the kinetics is mainly governed by the random walker's behavior in the vicinities of low-energy traps. That is, Fig. 6(b) reveals the fact that SELT's walker has a better memory, or, in other words, spends a longer time, on low-energy traps, which in turn implies lower probabilities of finding these traps (since both models share the same energy histogram [23]). Indeed, this deduction is echoed by the results of MFPT toward the second minima ($E = -20$), as listed in Table I, where the number from SELT simulations is almost 10 times longer than that from RCM.

In Table I we also list the equilibrium average energy at $T = 0.7$, for both SELT and RCM simulations. Note that while $\langle E \rangle$ is a time-averaged quantity, $\langle E \rangle'$ is an average over moves.

TABLE I. Average energies and MFPTs, for RCM and SELT at $T = 0.7$. For each model, the average energies are derived from a simulation of 10^{10} time steps. Unprimed data are time-averaged quantities, while primed data are averages over moves. Each MFPT value is obtained from 10 000 simulations.

	$\langle E \rangle$	$\langle E \rangle'$	MFPT	
			To $E = -24$	To $E = -20$
RCM	−22.7	−14.9	1.74×10^7	2.44×10^6
SELT	−23.0	−10.7	3.60×10^6	2.25×10^7

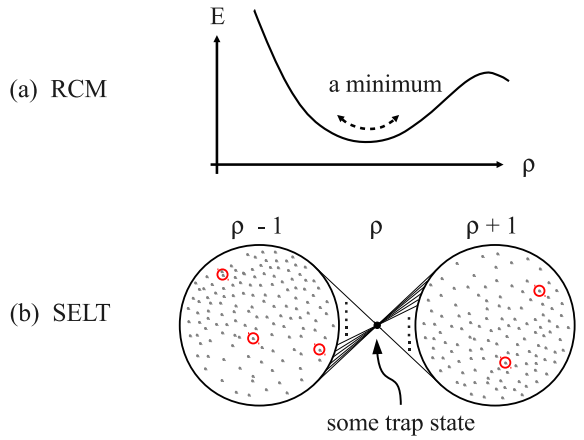

FIG. 7. (Color online) (a) Illustration for a deep energy minimum of RCM. (b) Illustration for a trap state of SELT. Circled dots represent the true-neighbor configurations. Links between ρ and $\rho \pm 1$ are represented by lines.

For both models, $\langle E \rangle'$ is less negative than $\langle E \rangle$. This is well understood, since the move-average treatment greatly reduces the weight carried by the minima, by overlooking the durations of the random walker's steadier stays on them. This effect is even more prominent for SELT, as shown clearly by the frozen stays in Fig. 5.

The MFPT results listed in Table I reveal a curious fact: while SELT's random walker finds the native state more quickly, the time it needs to get to a second minimum is even longer than the MFPT of RCM. On the contrary, the RCM random walker gets to a second minimum more quickly than its opponent gets to the native state. The implications of this comparison are derived in Sec. IV.

IV. DISCUSSION

What causes such different behaviors from the two models after all? In Fig. 7(a) we illustrate for RCM the landscape around a deep energy minimum. Due to the specificity of configuration links, around the minimum there exist gentle and definite energy steps. Once getting into the vicinity, the random walker moves in and out of the minimum frequently, as shown in our time-series result in Fig. 5.

As for SELT, we need to turn to another perspective, as illustrated in Fig. 7(b), for the specificity of configuration links is replaced by the random energy approximation. As an artifact, SELT combines various configurations into a supernode at each ρ. Standing on a "state" of ρ, the random walker is allowed to move onto any configuration of $\rho \pm 1$. In this way, a local minimum configuration in RCM might not remain a minimum when it is transformed to become a state in SELT yet can still serve as a trap dynamically. Conversely, a low-energy trap state in SELT might not correspond to minimum configurations when transformed back to RCM either (one major exception is the native state, being a minimum, and certainly the global minimum, in both models.) In Fig. 7(b) we show that in SELT the true-neighbor configurations are dramatically diluted in the $\rho \pm 1$ populations. Effectively, unlike the gentle and shallow energy steps toward these true neighbors, the stochastically generated steps are often steep and can confine the random walker straight in the trap.

To be specific, we now take a trap state of ($E = -20$, $\rho = 13$), for example. In SELT, all $18\,780\,864(\rho = 12) + 6624(\rho = 14)$ configurations are taken as its neighbors, whereas this trap state actually corresponds to 36 configurations in the RCM. Out of these 36 configurations, 24 are minima of the same class; each has 2 (out of the 12) true neighbors that provide low-energy steps of $\Delta E = +2$. The remaining 12 are minima of another class; each has 2 (of the 12) true neighbors that provide $\Delta E = +4$.

This example shows how slim the chance is to win the lottery of these low-energy true neighbors, as the random energy approximation effectively brings entropic difficulty to it. Still more, the numerous "virtual" neighbors enforced on the state are mostly unfavored energetically. When the random walker is eventually freed—either luckily, through the low-energy true neighbors, or via any (true or virtual) high-energy neighbor—once it is out, it can hardly find this trap again and therefore does not linger around. As reported in Table I, the chance of getting into the low-energy trap is as slim as that of getting out, and even slimmer than the chance of finding the native state.

The differences between the two models mainly lie in their walkers' distinct behaviors at secondary minima. The random walker of RCM wastes considerably more moves roaming around secondary minima. For example, at $T = 0.7$, during the FP to the native state, the number of moves taken by RCM's walker is two order of magnitude larger than that of SELT's (as shown in Fig 4), whereas the average number of FP moves to a secondary minima decreases to 8.7×10^3, in the same order as that of SELT (4.2×10^3).

The Rubik's cube model has such a network structure and numerous configurations, which make its energy landscape strikingly similar to those of complex macromolecules or other glassy systems [16,24]. The Monte Carlo simulations of RCM, instead of following clear pathways towards the native state, proceed like a randomly searching walker within the energy landscape. This dynamic behavior also mimics that of complex chemical reactions, which are often studied using SELT. However, we show in this work that the approach of using the random energy Hamiltonian, which is often adopted in SELT, fails to give a correct description for the dynamic behavior of RCM.

Contrary to the general thought that the randomness in the energy distribution results in a bumpy energy landscape and slow searching dynamics, we have demonstrated through the Rubik's cube problem that the random energy description leads to a faster dynamics instead. To our surprise, it is the lack of energy correlation that speeds up the searching process. Evidently derived from our results, these observations should provide insight into the essence of the random energy approach in studies of complex kinetics.

ACKNOWLEDGMENTS

This work was supported by the National Science Council of the Republic of China under Grants No. NSC-101-2112-M-008-001 and No. 99-2112-M-003-012-MY2. C.L.L. is grateful for support from the NCTS focus group Life and Complexity.

[1] D. R. Hofstadter, Sci. Am. **244**, 20 (1981).
[2] M. Davidson, J. Dethridge, H. Kociemba, and T. Rokicki (2010), http://www.cube20.org.
[3] The definition in the cited article [2] is slightly different from ours. For clarity, in our discussion, single steps are defined only for rotations by 90°. Rotations by 180° are combined operations, each accomplished by two steps of the same sense.
[4] D. Joyner, *Adventures in Group Theory: Rubik's Cube, Merlin's Machine, and Other Mathematical Toys*, 2nd ed. (Johns Hopkins University Press, Baltimore, MD, 2008).
[5] C. B. Anfinsen, Science **381**, 223 (1973).
[6] K. Kuwajima, Proteins Struct. Funct. Genet. **6**, 87 (1989).
[7] K. A. Dill and H. S. Chan, Proc. Natl. Acad. Sci. U.S.A. **90**, 1942 (1993).
[8] E. I. Shakhnovich, Curr. Opin. Struct. Biol. **7**, 29 (1997).
[9] N. Metropolis *et al*., J. Chem. Phys. **21**, 1087 (1953).
[10] J. N. Onuchic, Z. Luthey-Schulten, and P. G. Wolynes, Annu. Rev. Phy. Chem. **48**, 545 (1997).
[11] K. A. Dill and H. S. Chan, Nature Struct. Biol. **4**, 10 (1997).
[12] C.-L. Lee and M.-C. Huang, Eur. Phys. J. B **64**, 257 (2008).
[13] E. W. Montroll and K. E. Shuler, in *Advances in Chemical Physics, Vol. 1*, edited by I. Prigogine and P. Debye (John Wiley & Sons, Hoboken, NJ, 2007), pp. 361–399.
[14] R. Zwanzig, A. Szabo, and B. Bagchi, Proc. Natl. Acad. Sci. USA **89**, 20 (1992).
[15] J. D. Bryngelson and P. G. Wolynes, Proc. Natl. Acad. Sci. U.S.A. **84**, 7524 (1987).
[16] D. Sherrington and S. Kirkpatrick, Phys. Rev. Lett. **35**, 1792 (1975).
[17] B. Derrida, Phys. Rev. Lett. **45**, 79 (1980).
[18] J. D. Bryngelson and P. G. Wolynes, J. Phys. Chem. **93**, 6902 (1989).
[19] From our exhaustive computer search, a rotation of our definition would form a link only between ρ and $\rho \pm 1$, not within ρ or reaching any farther than $\rho \pm 1$.
[20] H. S. Chan and K. A. Dill, Proteins Struct. Funct. Genet. **30**, 2 (1998).
[21] C.-L. Lee, G. Stell, and J. Wang, J. Chem. Phys. **118**, 959 (2003).
[22] C.-L. Lee, C.-T. Lin, G. Stell, and J. Wang, Phys. Rev. E **67**, 041905 (2003).
[23] The energy probability distribution $P(E,\rho)$ and connecting probability $\lambda_{\pm}(\rho)$ are acquired from RCM and applied to SELT. In other words, the population distribution $n(E)$ in RCM is effectively inherited by SELT. Therefore, in simulations that reach quasiequilibrium, the fraction of time spent on certain energy should be the same for both models.
[24] S. Sastry, P. G. Debenedetti, and F. H. Stillinger, Nature **393**, 554 (1998).